

# Improved Flaw Detection and Characterization with Difference Thermography

William P. Winfree, Joseph N. Zalameda and Patricia A. Howell

NASA Langley Research Center MS 231, Hampton, VA 23681

## ABSTRACT

Flaw detection and characterization with thermographic techniques in graphite polymer composites is often limited by localized variations in the thermographic response. Variations in properties such as acceptable porosity, variations in fiber volume content and surface polymer thickness result in variations in the thermal response that in general cause significant variations in the initial thermal response. These variations result in a noise floor that increases the difficulty of detecting and characterizing deeper flaws. The paper investigates comparing thermographic responses taken before and after a change in state in a composite to improve the detection of subsurface flaws. A method is presented for registration of the responses before finding the difference. A significant improvement in the detectability is achieved by comparing the differences in response. Examples of changes in state due to application of a load and impact are presented.

**Keywords:** thermography, composites, flaw detection, nondestructive evaluation

## 1. INTRODUCTION

With the increased application of composites in commercial and military aircraft, rapid large area inspections are more important for ensuring the safety and reliability of aircraft. Graphite fiber reinforced composite materials are being used as primary structure due to their high stiffness and strength to weight ratio. One particular interest is the detection of delaminations that can appreciably reduce the compressive strength of a composite.

Thermography is a demonstrated technique for rapid inspections of materials and structures and has been shown to have great potential for detection of delaminations in composites.<sup>1-6</sup> These efforts have included a variety of heating and data reduction techniques to improve the detectability and assessment of the size and depth of delaminations.

Single sided thermographic detection of deeper delaminations in graphite fiber reinforced polymer(GFRP) composites is difficult.<sup>7</sup> There are three obvious reasons for this. The first reason is GFRP composites are an anisotropic material, with the fibers typically in the plane parallel to the surface. The high thermal conductivity of the graphite fibers relative to the thermal conductivity of the polymer results in the heat diffusing much faster in the direction of the fibers. The in-plane diffusion is much faster than the through the thickness diffusion, therefore the heat diffuses around deep flaws and does not result in a significant temperature increase at the surface. A second reason deep delaminations are difficult to detect is the inherent inhomogeneity of the GFRP composite. Small pockets of trapped air near the surface or variations in the fiber volume content results in variations in the surface temperature that can be as large as the variation caused by a delamination. Thirdly for depths close to the thickness of the composite, the maximum possible difference between the delaminated and undelaminated composite is proportional to the ratio of the thickness of the composite below the delamination to the total thickness above the delamination. As this thickness below the delamination goes to zero, so does the difference.

A fourth, perhaps less obvious reason deep delaminations are difficult to detect in composites is a result of the nature of delamination in the composites. Delaminations in composites are a thin air gap between two plies in

---

Further author information: (Send correspondence to William P. Winfree)

WPW.: E-mail: william.p.winfree@nasa.gov, Telephone: (757)864-4963

JNZ.: E-mail: Joseph.N.Zalameda@nasa.gov, Telephone: (757)864-4793

PAH.: E-mail: Patricia.A.Howell@nasa.gov, Telephone: (757)864-4786

the composite. If the thickness of the air gap is small, the heat flow across the gap may not provide a significant enough thermal resistance relative to the layer above the delamination. The effect of the thermal resistance on the thermal response of the delamination has been previously examined by several groups.<sup>8-10</sup> In Sec. 2, it is shown that the contact resistant of the delamination must be significant relative to the thermal resistance of the layer above it to be detectable.

This paper investigates the potential for increasing the detectability of flaws in composites by performing a “difference thermography.” For difference thermography, the thermal response of the composite is measured while the composite is in one state, referred to as a “baseline” measurement. The state of the composite is then changed and by carefully aligning the images corresponding to the thermal response with an affine transform, a point-by-point comparison of the thermal responses is made. By performing the affine transform on the data, the specimen and measurement system are not required to stay in fixed positions relative to each other for the baseline and post change-in-state measurements as was done previously.<sup>11</sup> Two examples are given, the first using a wedge to open an existing delamination to change the state of the composite. In the second example, the change in state is pre and post impact. For both cases, calculating the point-by-point state change induced difference in thermal response is shown to significantly improve the detectability of subsurface damage.

## 2. ONE DIMENSIONAL MODEL FOR COMPOSITE WITH DELAMINATION

A simple analytic solution does not exist for the one-dimensional heat flow in a multilayered material. The Laplace transform solution for two layers of thickness  $L_1$  and  $L_2$  coupled by an intermediate contact resistance( $R$ ) is known. Since the configuration of interest is a composite with a delamination, the first and second layers are assumed to have the same thermal conductivity ( $K$ ) and diffusivity ( $\alpha$ ). For the surface with the incident heating, the Laplace transform of the temperature response of the front surface ( $T_F(s)$ ) for instantaneous heating is given by<sup>12</sup>

$$\mathbf{M}_2 \begin{bmatrix} 1 & -R \\ 0 & 1 \end{bmatrix} \mathbf{M}_1 \begin{bmatrix} T_F(s) \\ f \end{bmatrix} = \begin{bmatrix} T_B(s) \\ 0 \end{bmatrix} \quad (1)$$

where

$$\mathbf{M}_i = \begin{bmatrix} \cosh(L_i \sqrt{s/\alpha}) & -\sinh(L_i \sqrt{s/\alpha}) / (K \sqrt{s/\alpha}) \\ -K \sqrt{s/\alpha} \sinh(L_i \sqrt{s/\alpha}) & \cosh(L_i \sqrt{s/\alpha}) \end{bmatrix}, \quad (2)$$

$T_B(s)$  is the Laplace transform of the back surface temperature and  $f$  is the incident flux. Solving for  $T_F(s)$  gives

$$T_F(s) = \frac{f\alpha(-2 + e_1(e_2(-2 + KR\sqrt{s/\alpha}) - KR\sqrt{s/\alpha}) + (e_1 - 1)KR\sqrt{s/\alpha})}{K((e_1 - 1)(e_2 - 1)KRs - 2(e_1e_2 - 1)\sqrt{s\alpha})} \quad (3)$$

where

$$e_1 = e^{-2L_1\sqrt{s/\alpha}} \quad (4)$$

$$e_2 = e^{-2L_2\sqrt{s/\alpha}}. \quad (5)$$

The Laplace transform for the difference between delaminated and undelaminated thermal responses( $R = 0$ ) is given by

$$T_d(s) = \frac{2\alpha e_1(e_2 - 1)^2 f R \sqrt{\frac{s}{\alpha}}}{(e_1 e_2 - 1) (KRs(e_1(-e_2) + e_1 + e_2 - 1) + 2\alpha(e_1 e_2 - 1) \sqrt{\frac{s}{\alpha}})}. \quad (6)$$

Note that the full thickness response is the reference being subtracted and not the Laplace transform of a semi-infinitely thick thermal response media to instantaneous heating or  $f\sqrt{\alpha/s}/K$ .

A simple analytical solution for the inverse Laplace transform of Eq. 3 does not exist, however if one assumes the contact resistance is small, then the time response is given by

$$T_F(t) = \frac{f}{K} \sqrt{\frac{\alpha}{\pi t}} \left[ 1 + 2 \sum_{n=1}^{\infty} e^{\frac{-n^2 L^2}{\alpha t}} + \frac{KR}{L_1} G(t, p) + O(R^2) \right] \quad (7)$$

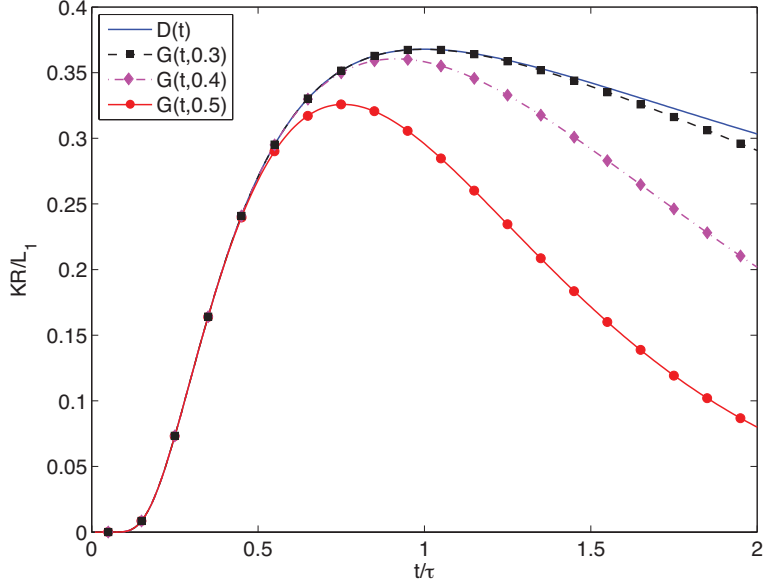


Figure 1. Time dependence  $D(t)$  as expressed in Eq. 9 which gives relative change in the thermal response of a composite due to a delamination if the contact resistance of the delamination is small relative to the thermal resistance of the layer above it. For comparison, the full series solution( $G(t, p)$ ) for different values of  $p$  are also plotted.

where

$$G(t, p) = \frac{p^2 L^2}{t\alpha} \sum_{n=1}^{\infty} n \left( -2ne^{-\frac{n^2 L^2}{\alpha t}} + (n-p+1)e^{-\frac{L^2(n-p+1)^2}{\alpha t}} + (n+p-1)e^{-\frac{L^2(n+p-1)^2}{\alpha t}} \right) \quad (8)$$

and  $L_1 = pL$  and  $L_2 = L(1-p)$  with  $L$  being the full thickness of the composite. The first two terms inside the bracket correspond to the thermal response of a layer with no delamination. The third term is the difference between the single layer response and the response with a delamination. This term must be significant, relative to 1 for the delamination to produce a significant change in the thermal response of the composite. If  $p < 0.3$  (delamination is in top half of the specimen), to a good approximation, this third term can be further simplified to

$$D(t) = \frac{KR\tau}{L_1} \frac{1}{t} e^{-\frac{\tau}{t}} \quad (9)$$

where  $\tau = \alpha/L_1^2$ . The time dependence of  $D(t)$  is shown in Fig.1.  $D(t)$  has a maximum value at  $t = \tau$  of  $e^{-1}$  times  $KR/L_1$ , which is the ratio of thermal resistance of the layer above the delamination to the contact resistance. After reaching this maximum, since the contact resistance is small, the heat flows through the delamination. This reduces the front surface temperature to the value for no delamination without requiring any heat flow around the delamination. For deeper delaminations, the effect of the delamination is reduced since  $L_1$  is greater and  $G(t, p)$  has a lower maximum value.

### 3. METHOD FOR REGISTRATION OF TWO THERMAL RESPONSES

The two thermal responses can be considered to be a series of images,  $A_i(x, y)$  and  $B_i(x, y)$ , where  $i$  corresponds to time of the image and  $x$  and  $y$  correspond to the location of pixels in the image. To register the two thermal data sets, the first unsaturated thermal images (defined as  $i = 1$  for each thermal response) are registered to each other. For the cases examined, the baseline data sets are held fixed and the data sets from post change are transformed for registration with the initial state. For many cases a simple rotation and translation is required. However, it is possible that between the data acquisition, the configuration could have changed enough that the plane of the specimen is in a plane that is rotated relative to initial configuration. For those cases, an affine transform is required.

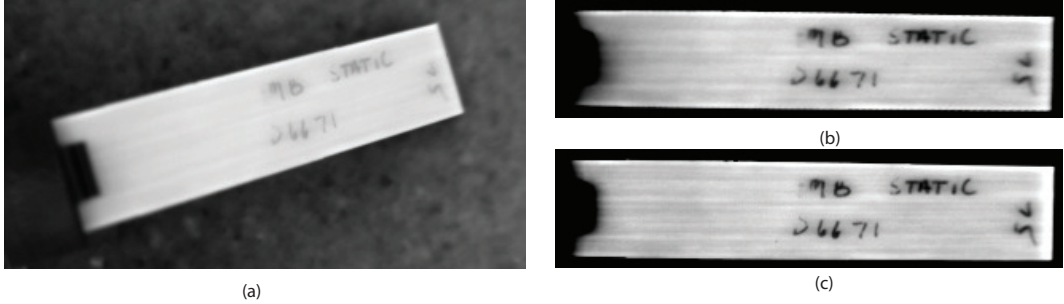


Figure 2. Registration of images based on affine transform. (a) Infrared image of specimen tilted out of the normal plane of data acquisition by approximately 30° and rotated by approximately 16°. (b) Results of the affine transform using  $\Psi$ . (c) Fixed reference infrared image with tilt  $\approx 0$  and rotation  $\approx 0$  that was the target of the optimization routine.

The affine transform is given by

$$\begin{bmatrix} a_{1,1} & a_{1,2} & a_{1,3} \\ a_{2,1} & a_{2,2} & a_{2,3} \\ 0 & 0 & a_{3,3} \end{bmatrix} \begin{bmatrix} x \\ y \\ 1 \end{bmatrix} = \begin{bmatrix} x' \\ y' \\ 1 \end{bmatrix} \quad (10)$$

where  $x$  and  $y$  are the coordinates of the initial frame of reference and  $x'$  and  $y'$  are the coordinates of the transformed frame of reference. The elements of the matrix,  $(a_{1,1} \dots a_{3,3})$  are seven independent parameters which represent the affine transform.

When the transformation is a simple rotation by  $\theta$ , followed by a translation of  $x_t$  and  $y_t$  and finally a scaling then Eq.10 becomes

$$\begin{bmatrix} \cos(\theta) & \sin(\theta) & x_t \\ -\sin(\theta) & \cos(\theta) & y_t \\ 0 & 0 & 1/m \end{bmatrix} \begin{bmatrix} x \\ y \\ 1 \end{bmatrix} = \begin{bmatrix} x' \\ y' \\ 1 \end{bmatrix} \quad (11)$$

where  $m$  is the magnification.

Registration of the two thermal responses is performed by selecting a region on interests in  $A_1(x, y)$ . To determine the proper value for  $\psi = [a_{1,1}, a_{1,2}, a_{1,3}, a_{2,1}, a_{2,2}, a_{2,3}, a_{3,3}]$ , initial values are chosen for the different elements of  $\psi$  and image  $B_1(x, y)$  is transformed to  $C_1(x, y)$ . The pixels of  $C_1(x, y)$  that correspond to the pixels of the region of interest in  $A_1(x, y)$  are amplitude and offset matched using a least squares estimation. The sum of the squared differences of the least squared estimation is used as the cost for a simulated annealing routine that varies  $\psi$  to determine  $\Psi$ , the value of the vector corresponding to the global minimum for the cost. The  $\Psi$  is then used as the parameters for performing the affine transform of  $B_i(x, y)$  for  $i = 1$  to  $N$  (number of images) to  $C_i(x, y)$ .  $A_i(x, y)$  is then subtracted from  $C_i(x, y)$  for  $i = 1$  to  $N$  to calculated the difference thermography data set.

An example of the results of this process is shown in Fig.2. A composite specimen with a wedge insert into a delamination was tilted out of the typical measurement plane by approximately 30° and rotated by approximately 16°. This should be considered to be an undesirable initial alignment, however, it is presented as a demonstration of the capability of the registration technique. As can be seen in Fig.2, the registration technique results in an image that has excellent image registration with the target image. The technique resulted in excellent registration for all cases considered.

#### 4. APPLICATION OF DIFFERENCE THERMOGRAPHY TO COMPOSITE SPECIMENS

Difference thermography was applied to two different types of composite damage. The first type of damage examined was an existing delamination with and without a wedge insert into the delamination to increase the gap width. The second type of damage was impact damage, where the difference was taken between pre and post impact data.

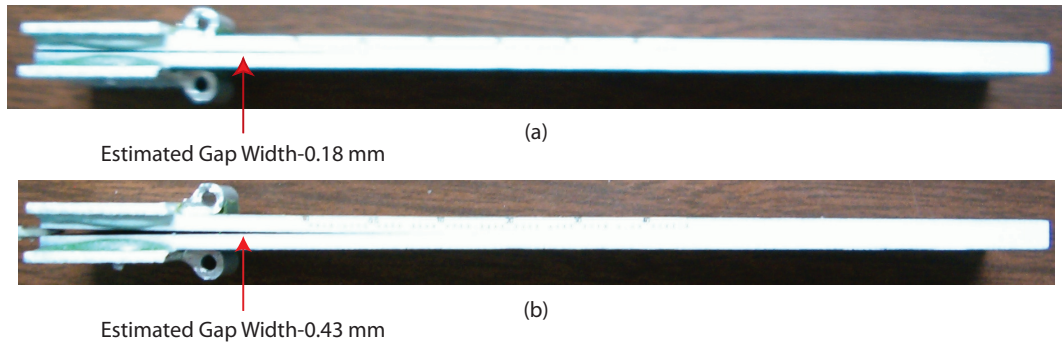


Figure 3. Side view of the composite specimen discussed in Sec. 4.1. (a) The composite specimen with existing delamination. (b) Same specimen with wedge inserted into the delamination. The estimated width of the air gap is shown at the same point of the specimen.

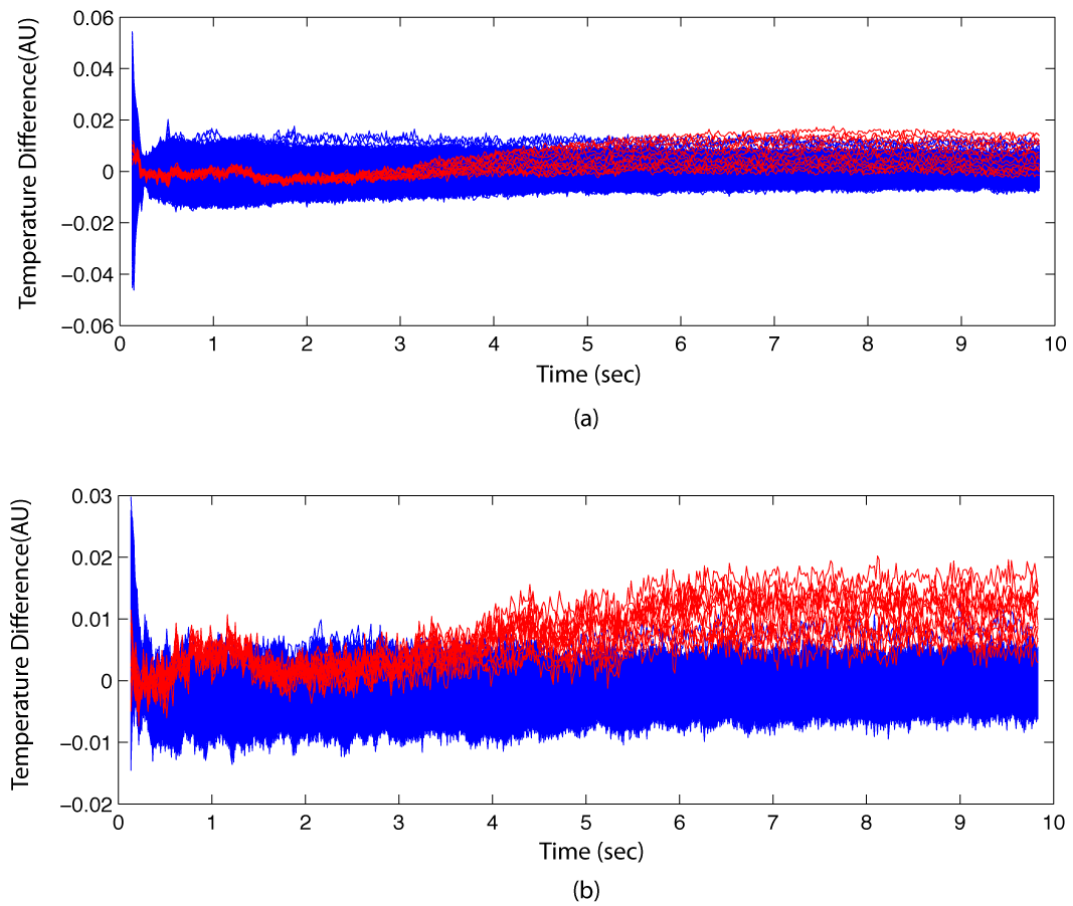


Figure 4. Difference between thermal response of composite with wedge opening delamination and reference. (a) Reference is the mean of the thermal response of in a region without delamination. (b) Reference is point in the aligned thermal thermal response, taken before delamination is widen with wedge. For both (a) and (b), the difference signals acquired from the undamaged region of the specimen is shown in blue and difference signals from the delaminated region is shown in red.

#### 4.1 Composite with delamination

The first case examined was a composite specimen with an existing delamination. A picture of the side of the composite with and without the wedge inserted is shown in Fig. 3. As can be seen from the figure, the width of the air gap decreases as one moves from the left side of the image toward the middle of the specimen. At the points with the estimated gap widths,  $RK/L_1 \approx 3$  for Fig. 3(a) and  $RK/L_1 \approx 8$  for Fig. 3(b).

After performing the image registration as discussed in Sec. 3, the point-by-point differences in the thermal response were calculated. A comparison of two methods for calculating the difference in thermal response are shown in Fig. 4. For both Fig. 4(a) and Fig. 4(b), the data shown are from the composite with a wedge inserted into the delamination. Fig. 4(a) displays the difference between thermal responses and a reference calculated from the mean value at each time in a region of the composite where no delamination exists. The red response difference signals are from the delaminated region of the composite and the blue difference signals are from the undamaged region of the composite. As can be seen from the figure, even with the significant increase in gap width, there is considerable overlap between the difference signals of delaminated and undelaminated regions for all times.

Instead of using a single reference single, the difference signals were calculated from the signals of the registered data sets from prior to and post insertion of the wedge into the delamination. The results are shown in Fig. 4(b). By differencing baseline and registered post thermal responses, the variability of the undelaminated region of the specimen is significantly reduced. This results in a difference response for the delaminated region that is greater than the variability of the undelaminated region from approximately 5 seconds to the end of the time record at 10 seconds.

Averages of the thermal responses of the composite from 3 to 5 seconds with and without the wedge in the delamination are shown in Fig. 5(a) and Fig. 5(b) respectively. When there is no wedge inserted into the delamination, it is difficult to detect the delamination in the averaged thermal response. After inserting the wedge, the delamination is more obvious in the image, however, it is difficult to establish where the edge of the delamination is. There is a gradual change in the response as one moves from the undelaminated to delaminated region of the composite.

The averaged response obtained by calculating the difference of the registered thermal responses for prior to and post insertion of the delamination is shown in Fig. 5(c). As can be seen from this figure, the differencing of the thermal responses considerably improves the visualization of the delaminated region. It is also much more evident where the delamination ends on the specimen.

If one assumes the baseline thermal response of the composite is approximately the thermal response of the undelaminated composite, then one can use Eq. 6 to estimate the depth of the delamination from the difference response. The inversion of Eq. 6 is performed numerically using the Talbot method.<sup>13</sup> One of the unknowns in Eq. 6 is  $R$ , however for large gap thicknesses ( $\sim 0.01$  cm or  $RK/L_1 \sim 2$ ), the shape of the thermal response is not very dependent on the value of  $R$  for times less than  $\tau \sim 20$  second, therefore  $RK/L_1$  was set to 2. The good agreement of model and data is shown in Fig. 6. From fits of a significant portion of the delaminated region, the depth of delamination from the thermal fit was estimated to be  $0.22 \pm 0.02$  cm which is in agreement with the depth of delamination from the measurement of the specimen of 0.219 cm.

#### 4.2 Composite with impact damage

A second case examined was a composite structure undergoing impact testing. Baseline and post impact data were acquired on the structure. The first unsaturated images of the two data sets were registered using the method discussed in Sec. 3, then the point-by-point differences in the thermal response were calculated. There were reference marks on the surface of the composite, however they were not required to register the data sets, since the initial images had significant variations due to local anomalies in the composite. The markings were intended to indicate where the composite was to be impacted.

For one of the impacted regions, the thermal indications of impact damage for this case are not significantly larger than the normal variations in the composite as can be seen by comparing Fig. 7(a) and Fig. 7(b). When the difference thermography image is examined (Fig. 7(c)), the impact damage becomes the predominate feature in the image. What also becomes obvious is damage that is not visible without performing the difference

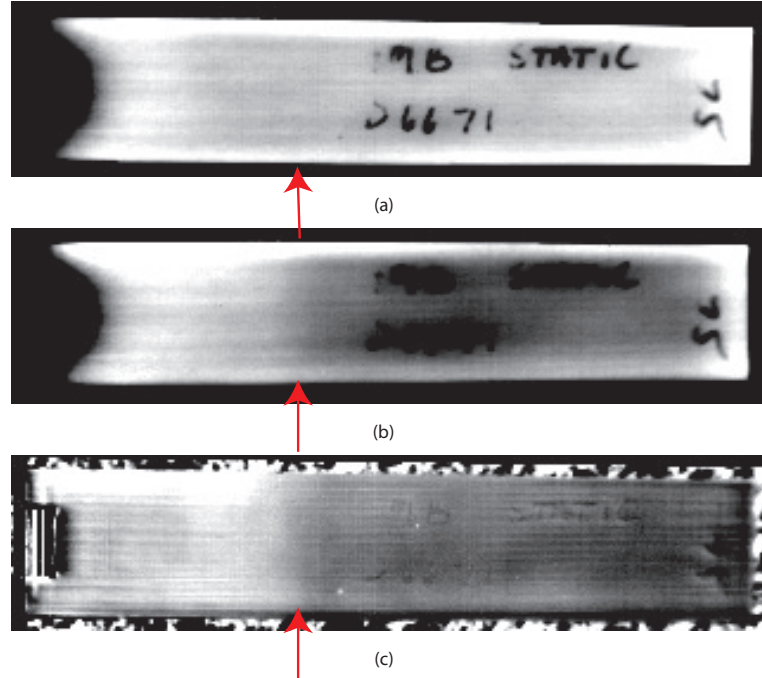


Figure 5. Average from 3 to 5 seconds of singled sided thermal response. (a) Results of the averaged signal for composite without wedge in delamination. (b) Results of the averaged signal for composite with wedge in delamination. (c) Results of the difference between the thermal response of the same specimen with and without the delamination gap increased. Arrow indicates the approximate end of the delamination, based on examination of the edge of the composite.

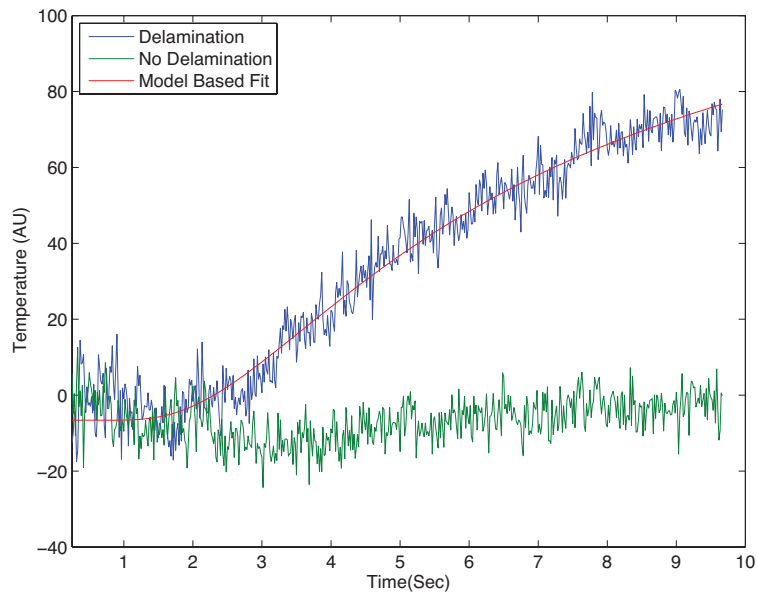


Figure 6. The difference between thermal responses with and without the delamination gap widened for point over delamination and point over no delamination. The fit of the delamination data based on Eq. 6 is overlaid on the delamination response.

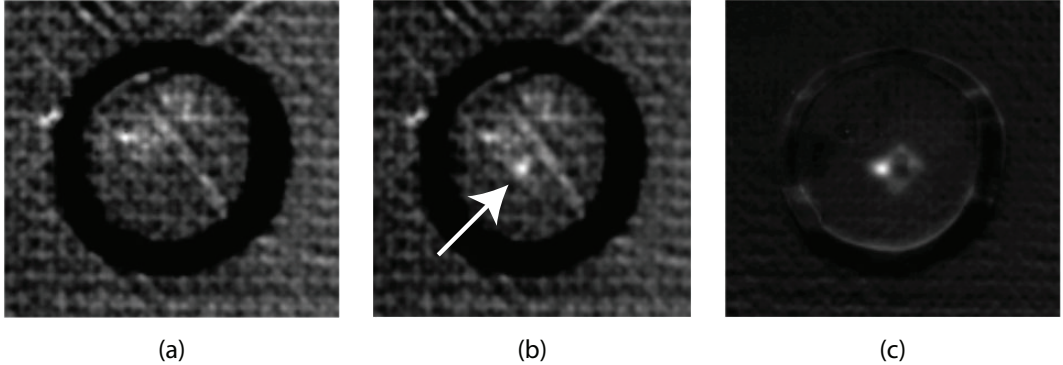


Figure 7. Results of difference thermography technique for impacted specimen. (a) Infrared image of region of structure taken prior to impact. (b) Infrared image of same region taken after impact. (c) Difference image of region at 0.5 second following flash heating taken prior to impact. All images represent data at 0.5 second following flash heating.

thermography. The depth of the damage was not determined from this data, due to the small lateral size of the damage.

## 5. SUMMARY

Difference thermography is shown to be an effective method for improving the detectability of flaws in a composite. Two examples are discussed, the first using a wedge to open an existing delamination to change the state of the composite and the second the change in state is pre and post impact. For both cases, the difference thermography is shown to significantly improve the detectability of subsurface damage. An affine transform of infrared images enabled registration of the thermal response without requiring the specimen and measurement system stay in fixed positions relative to each other for the prior to and post change in state measurements.

## REFERENCES

- [1] Almond, D., Delpech, P., Beheshtey, M., and Wen, P., "Quantitative determination of impact damage and other defects in carbon fiber composites by transient thermography," in *[Nondestructive Evaluation of Materials and Composites]*, S.R. Doctor, C.A. Lebowit, G. B., ed., *Proc. SPIE* **2944**, 256–264 (1996).
- [2] Ball, R. J. and Almond, D. P., "The detection and measurement of impact damage in thick carbon fibre reinforced laminates by transient thermography," *NDT & E International* **31**(3), 165 – 173 (1998).
- [3] Plotnikov, Y. and Winfree, W., "Temporal treatment of a thermal response for defect depth estimation," in *[Review of Progress in Quantitative NDE]*, Thompson, D. O. and Chimenti, D. E., eds., *AIP Conf. Proc.* **509**, 587–594 (2000).
- [4] Rajic, N., "Principal component thermography for flaw contrast enhancement and flaw depth characterization in composite structures," *Composite Structures* **58**(4), 521 – 528 (2002).
- [5] Avdelidis, N. P., Hawtin, B. C., and Almond, D. P., "Transient thermography in the assessment of defects of aircraft composites," *NDT & E International* **36**(6), 433 – 439 (2003).
- [6] Avdelidis, N. P., Almond, D. P., Marioli-riga, Z. P., Dobbington, A., and Hawtin, B. C., "Pulsed thermography: philosophy, qualitative & quantitative analysis on aircraft materials & applications," in *[Proc. Vth International Workshop, Advances in Signal Processing for Non Destructive Evaluation of Materials]*, Maldague, X., ed., 171–179 (2006).
- [7] Meola, C., Carluomagno, G. M., and Giorleo, L., "Geometrical limitations to detection of defects in composites by means of infrared thermography," *Journal of Nondestructive Evaluation* **23**, 125–132 (2004). 10.1007/s10921-004-0819-z.
- [8] Bendada, A., "Approximate solutions to three-dimensional unsteady heat conduction through plane flaws within anisotropic media using a perturbation method," *Modelling and Simulation in Materials Science and Engineering* **10**(6), 673–684 (2002).

- [9] Winfree, W. P. and Zalameda, J. N., "Thermographic determination of delamination depth in composites," in [*Thermosense XXV*], Cramer, K. E. and Mal dague, X., eds., *Proc. SPIE* **5073**, 363–373 (2003).
- [10] Badghaish, A. A. and Fleming, D. C., "Non-destructive inspection of composites using step heating thermography," *Journal Of Composite Materials* **42**(13), 1337–1357 (2008).
- [11] Shepard, S. M., "Method and apparatus for detecting kissing unbonded defects," *Patent US 7,083,327 B1* (2006).
- [12] Carslaw, H. S. and Jaeger, J. C., [*Conduction of Heat in Solids*], Oxford University Press, New York, NY (1986).
- [13] Cohen, A. M., [*Numerical Methods for Laplace Transform Inversion*], Springer, New York, NY (2007).